Available online at www.sciencedirect.com

ScienceDirect

journal homepage: www.elsevier.com/locate/issn/15375110

Research Paper

Finite element method model of the mechanical behaviour of *Jatropha curcas* L. bulk seeds under compression loading: Study and 2D modelling of the damage to seeds

Michal Petrů [a,*], *Ondřej Novák* [b], *David Herák* [c], *Ivan Mašín* [d], *Petr Lepšík* [d], *Petr Hrabě* [e]

[a] *Institute for Nanomaterials, Advanced Technologies and Innovation, Technical University of Liberec, Liberec, Czech Republic*
[b] *Department of Nonwovens, Faculty of Textile Engineering, Technical University of Liberec, Liberec, Czech Republic*
[c] *Department of Mechanical Engineering, Faculty of Engineering, Czech University of Life Sciences Prague, Prague, Czech Republic*
[d] *Department of Design of Machine Elements and Mechanisms, Faculty of Mechanical Engineering, Technical University of Liberec, Liberec, Czech Republic*
[e] *Department of Material Science and Manufacturing Technology, Faculty of Engineering, Czech University of Life Sciences Prague, Prague, Czech Republic*

ARTICLE INFO

Article history:
Received 13 November 2013
Received in revised form
21 July 2014
Accepted 20 August 2014
Published online 15 September 2014

Keywords:
Linear compression loading
Visualisation
FEM
Volumetric strain
Superstructure
Biodiesel

This article is focused on comprehensive research of a pressing process of *Jatropha curcas* L. bulk seeds during linear compression. Compression experiments were performed and the strain and brittle fracturing of the seeds visualised. The mechanical behaviour and stress distribution at the volumetric strain of bulk seeds in pressing cylinders and semi-cylinders with diameters of 60, 80 and 100 mm were described by 2D FEM models. It has been determined that the study of nonlinear visco-elastic and plastic strain seed interactions and the damage and crack growth in such seeds can be significantly improved through computer simulations using an explicit FEM algorithm. In this study, the compressibility of ripe *J. curcas* L. bulk seeds was analysed and compared depending on the volume strain and energy performance of the linear pressing process. Empirical equations and differential deformation theory describing the seeds interacting beyond the oil point were reported. In addition, the issue of contact theory in numerical modelling of the point contact of interacting seeds was also described. Statistical results showed that the 2D FEM model can be used to study the volumetric strain, stress and damage of *J. curcas* L. bulk seeds. These studies suggest that FEM models may be considered an important tool to assess the energy performance of the pressing process of *J. curcas* bulk seeds and can provide valuable information for the design and optimisation of pressing equipment.

* *Corresponding author.*
E-mail address: michal.petru@tul.cz (M. Petrů).
http://dx.doi.org/10.1016/j.biosystemseng.2014.08.011

Nomenclature

a_S	area of contact, mm^2
A_D	force coefficient of mechanical behaviour, N
B_D	deformation coefficient of mechanical behaviour, mm^{-1}
C_n^{crit}	critical value of the normal contact stiffness, N mm^{-1}
C_S	coefficient of material stiffness, –
d	diameter of pressing cylinder, mm
E	initial elastic modulus, MPa
F	pressing force, N
$F(\sigma)$	Von Mises plasticity conditions, MPa
F_D	compressive force, N
F_n	normal force, N
F_T	contact force in a tangential direction, N
g	gravitational acceleration, m s^{-2}
G	initial shear modulus, MPa
H	height of the seed, mm
h	parameter of strain, –
K	initial bulk modulus, MPa
$L_{element}$	size element, mm
m_s	mass of the seed, kg
Δn_E	fractional size of the overlap elements, mm
p_S	surface pressure, MPa
R	radius of the seed, mm
S	projected area of the seed, mm^2
T	temperature, °C
t	time, s
t_0	initial time, s
Δt	time step, s
Δt^{crit}	critical value of the time step, s
v_S	speed of the seed movement, m s^{-1}
$V_{seeds,vessel}$	volume of seeds, or vessel, m^3
W	compression energy, J mm^{-3}
x	displacement, mm
γ	volumetric strain, –
δ	size of compression, mm
ε_{SS}	strain in the superstructure, –
$\varepsilon_{PP,C}$	strain in the piston, cylinder, –
$\dot{\varepsilon}_S$	strain rate, –
$\dot{\varepsilon}_S^P$	rate of plastic deformation, –
$\dot{\varepsilon}_S^E$	rate of elastic deformation, –
Λ, Γ	restrictive conditions for inequality, equality, –
λ_C	contact coefficient, MPa mm
μ	packing density, –
μ_{SS}	packing density of superstructure, –
μ_S	seed/seed friction, –
ν	Poisson ratio, –
ξ	compression factor, –
ρ	density, kg m^{-3}
σ_e	equivalent stress, MPa
σ_i	principal stress, MPa
σ_S	stress in the structure, MPa
σ_S^E	stress of the elastic component, MPa
σ_S^P	stress of the plastic component, MPa
σ_S^η	stress in the oil viscosity component, MPa
$\sigma_S^{\mu_S}$	stress in the friction component, MPa
$\sigma_{PP,C}$	stress in the piston, cylinder, MPa
σ_{SS}	stress in the superstructure, MPa
$\overline{\sigma}$	yield stress, MPa
τ	shear friction, –
χ	porosity, –
ψ, ϑ	dimensionless constants, –
Ω_{ripe}	initial geometry, –

1. Introduction

New knowledge, based on comprehensive interdisciplinary understanding of the nonlinear mechanical behaviour of crops and oilseeds in the pressing process (Adeeko & Ajibola, 1990; Connelly & Kokini, 2007; Emin & Schuchmann, 2013; Karaj & Müller, 2011, Khan & Hanna, 1983; Lim, Hoong, Teong, & Bhatia, 2010; Makkar, Francis, & Becker, 2008; Stefan, Ionescu, Voicu, Ungureanu, & Vladut, 2013) can improve theories and will contribute to optimisation and innovation of pressing equipment. In order to optimise devices, a deeper understanding of the complex behaviour of the compression process, which is influenced by the self-organised movement of seeds due to their mutual interactions, is required. This phenomenon is very difficult to describe in terms of understanding the resulting mechanical behaviour. Beyond the oil point, it can be observed that the efficiency of the moulding process is significantly affected by the friction, non-uniform porosity and viscosity of the individual seeds, which in turn causes the reorganisation of the visco-plastic deformation of the seeds. Deeper knowledge and a better understanding of this process, which is characterised by seed interactions during the pressing process beyond the oil point, could significantly contribute to the improvement of machinery and production equipment for seed pressing. Pressing of the structure with subsequent plastic deformation depends on the velocity and direction of the strain and affects the extrusion of *Jatropha curcas* L. oil (Addy, Whitney, & Chen, 1975; Blahovec & Řezníček, 1980; Koegel, Fomin, & Bruhn, 1973; Fomin, 1978; Herak, Gurdil, Sedlacek, Dajbych, & Simanjuntak, 2010; Herak, Kabutey, Petru, Hrabe, Lepsik, & Simanjuntak, 2014; Petrů, Novák, Herák, & Simanjuntak, 2012). The strain character depends on the effective strain rate, as can be found in practically all oil bearing crops (Akinosho, Raji, & Igbeka, 2009; Herak, Kabutey, Divisova, & Simanjuntak, 2013; Sukumaran & Singh, 1989). The process behaves elastically to a certain level of strain and subsequently plasticisation occurs, which gradually causes permanent deformation. Crack initiation and growth occur in the seed with the highest degree of strain. This problem, which manifests itself in the form of nonlinearity and anisotropic strain, has yet to be adequately described analytically. Theory and various empirical relationships describing the solution of critical material failure and subsequent crack growth can be found in many studies focused on materials with elastic–-plastic damage (Hinton, Kaddour, & Soden, 2004; Krajcinovic,

1996). Some studies have been focused directly on seed deformation. For example Ma, Cholewa, Mohamed, Peterson, and Gijzen (2004) explain that the size of the bulk seed porosity is a key factor for the rate of crack growth because if the porosity limit reaches zero, then the bulk seeds become non-porous and under normal conditions they are mechanically more durable. In addition, Dobrzanski and Stepniewski (2013) report that the seed in the initial stage of deformation has visco-elastic properties that gradually cause an increase in the internal pressure until sudden plastic failure occurs. The problem is that the experimentally obtained empirical relationships are typically limited to specific information and do not accurately describe the cause of this critical situation. Knowledge of the origin and distribution of plastic damage, which results in the critical limit compressibility being exceeded, is important especially when more seeds are compressed together. The formation of cracks in one seed influences the total energy efficiency of the compression process and the effective efficiency of the pressing technology because not only the structure of seeds but also the oil viscosity and volume of air in the individual parts of the pressing vessel cause non-homogeneous mechanical resistance against compression of the seeds. This is reflected in an uneven energy intensity of the pressing process. This phenomenon can be partly eliminated by the use of pressing equipment with variable geometry. Numerical methods such as FEM (finite element method) and DEM (discrete element method) can be applied for a deeper analysis of this complex process. Also, special methods utilising the principle of FEM with variable geometry like FDM (Fictitious Domain Methods) and IB-BCE (Immersed Boundary – Body Conformal Enrichment) can be applied. Almost all of the physical processes can be solved using numerical methods (Dekys & Broncek, 2012; Petrů & Novák, 2010; Petrů, Novák, & Lepšík, 2014). The difficulty lies in the time-consuming calculation of highly complex and nonlinear problems. In this case, the calculation time can only be reduced by using supercomputers. Therefore, in the case of very complex nonlinear processes, a simplified 2D model can be solved more effectively. For these processes, cross-sections selected based on the model symmetry can significantly shorten the calculation and the results can be close to the experimental values. The use of 2D simulations can also help to reduce computation time for a very high strain rate. The acquired knowledge can be valuable for the optimisation of machine parts and equipment (Connelly & Kokini, 2003; Petrů, Novák, Ševčík, & Lepšík, 2014; Petrů, Novák, Vejrych, & Lepšík, 2013; Vyakaranam & Kokini, 2011). The kinematics of granules in an orifice with different cross-sections have been studied with numerical simulations using DEM (Rong, Negi, & Jofriet, 1995). Previously published studies indicate that the kinetics of the relative movement of the granules are influenced by contact shear friction as previously reported by Bardet and Proubet (1991). Raji and Favier (2004) describe the DEM theory of compressing oil bearing crop seeds, in which experiment is compared with model simulations at a volumetric strain of 19% and deformation of 12 mm. The authors stated that the data determined from the model of the visco-elastic deformation was in very good conformity with the experimental data. For a kinetic description of the particles, which were stirred by two screws, they prepared a 2D numerical simulation using a mixed FEM Galerkin method. The model simulations reflect the shear stress caused by friction between the stirred particles. The results show that efficient stirring occurs if there are areas of so-called poor mixing (Connelly & Kokini, 2007). Kabas, Celik, Ozmerzi, and Akinci (2008) studied the mechanical properties of the kinetic impact of a falling apple and they claim that the internal stresses caused by the external forces immediately after impact are difficult to measure. Therefore, it is appropriate to establish a FEM analysis where, for increasing instantaneous stress, it is important to evaluate the strain in short intervals. A study of the deformation of bulk seeds during compression can also be based on models of the mechanical behaviour of another type of granule on a macro and micro level. The granules can be characterised as a mathematical set of macroscopic particles defined by their shape. Apparently different granulates, such as nuts in a pressing vessel or coal in the hopper of a crusher, have been described using this approach. Petrakis and Dobry (1989), and Petrakis, Dobry, and Ng (1988) dealt in their work with micromechanical studies and modelling of soil and sand behaviour using nonlinear FEM and DEM. The authors state that, from the results of both types of simulation, the most important role during deformation is played by the shear during mutual contact of the particles. The use of the particle photoelasticity technique showed stress chains in a cross-section of sand grains. These stress chains are formed under the influence of the external forces (Geng, Howell, Longhi, & Behringer, 2001). This shows that the spatial arrangement and shear of the grains can be considered as a key factor in the force reaction of compressed seeds. The aim of this article is to study the complex mechanical behaviour of regularly arranged *J. curcas* L. bulk seeds during linear compression in a closed pressing vessel which was adjusted for visual control of the whole compression process and for subsequent comparison and refinement of the FEM model through model simulations.

2. Materials and methods

2.1. *Background of theory*

Nonlinear behaviour with significant geometric deformation can be observed during the linear compression of individual *J. curcas* L. seeds at different stages of maturity (unripe, ripe, over-ripe) (Herak, Gurdil, Sedlacek, Dajbych, & Simanjuntak, 2010; Herak, Kabutey, Divisova, & Simanjuntak, 2013; Kabutey, Herák, Chotěborský, Dajbych, Divišová & Boatri, 2013; Petrů, Novák, Herák, & Simanjuntak, 2012). The characteristics of the bulk seeds are determined by porosity χ, density ρ(kg m^{-3}), volume deformation γ and temperature T (°C), deformation δ (mm), strain rate $\dot{\varepsilon}_S$, which can be transformed into elastic strain rate $\dot{\varepsilon}_S^E = f(\dot{\varepsilon}_S)|_{\leq \text{low oiliness point}}$ and plastic strain rate $\dot{\varepsilon}_S^P = f(\dot{\varepsilon}_S)|_{\geq \text{low oiliness point}}$. The maturity of the seeds affects the modulus of elasticity E (MPa), which is a function of strain and stress $E = f(\varepsilon_S, \sigma_S)$. Stress σ_S is formed of the elastic components of stress σ_E^S, yield stress $\bar{\sigma}$ and visco-plastic stress $\sigma_S^P = f(\sigma_S^\eta, \sigma_S^{\mu_S})$, where σ_S^η represents an element of the viscous stress tensor and $\sigma_S^{\mu_S}$ is an element of the frictional stress tensor. With increasing seed compression,

especially near to the oil point, the strain will be higher and can therefore be assumed (Petrů, Novák, Herák, & Simanjuntak, 2012) to be:

$$\sigma_S^E = f(\varepsilon_S^E)\big|_{\leq \text{low oiliness point}} \rightarrow \overline{\sigma} \leq \sigma_S^P = f(\varepsilon_S^P)\big|_{\geq \text{low oiliness point}}$$

The study and compilation of multi-seed strain compression theory for linear compression is more complex because interaction and transformation of the seeds are affected by other parameters, which need to be introduced into the mechanical system. The real pressing process is different from single seed compression in the creation of stress concentrators that occur on contact between the seeds. This is mainly due to the geometric arrangement of the entire granular system, mutual interactions and seed kinetics. Also, the differences in seed maturity lead to different mechanical properties. For the study, a mathematical description of the ideal case of isothermal compression has been introduced. Before compression, when deformation $\delta = 0|_{t=0}$, the pressing cylinder is filled with seeds in a manner that secures an ideally arranged granular system with minimal surface porosity (triangular arrangement with cross-section packing density $\mu \sim 0.91$) in the sectional plane. Consequently, the minimum potential energy of the system can be assumed. If a square arrangement is applied then the packing density will be $\mu \sim 0.78$. The section is made so that all of the seeds have the same cross-section, as shown in Fig. 1.

2.2. Study of the interaction of seeds in mutual contact

In the model according to Fig. 1 the maximum sum of all of the internal stresses of the individual seeds $\sum_i \sigma_{Si}\Big|_{i=1,2,\ldots,n}$ depends on the loading given by the weight of the individual seeds $\sum_i m_{Si}\cdot g\Big|_{i=1,2,\ldots,n} \rightarrow \max\sum_i \sigma_{Si}\Big|_{i=1,2,\ldots,n}$. After an initial compression of min $\delta \neq 0|_{t\neq 0}$ the seeds begin to reorganise gradually in a heterogeneous system up to the maximum compression $\delta \rightarrow \delta_{max}$ which leads to a complete collapse of the structure. This results in a mechanical system in which the sum of the internal stresses on each seed becomes a function of the strain of the gradually deforming seeds depending on the actual total packing density μ, whereas the immediate value of maximum compression $\delta = h_{max}|_{\mu_{lim\rightarrow 1}} \rightarrow \max\sum_i \sigma_{Si}\Big|_{i=1,2,\ldots,n} = \max\sum_i f(\varepsilon_{Si})\Big|_{i=1,2,\ldots,n}$ is crucial. The stress concentration on the outer boundary of the seeds becomes an important parameter of the compression energy $W = W(\varepsilon_{Si})|_{i=1,2,\ldots,n}$ which depends on the strain ith of the pressed seed and is affected by an increase in the contact factor of the interacting seeds λ_C [MPa mm] expressed by Eq. (1). This factor depends on the surface properties given by the shear friction τ, surface pressure p_S, and the amount of adhesion at the contact of the seeds, which is also affected by seed viscosity.

$$\lambda_C = 2\pi R \tau p_S\big|_{T=\text{const}} \tag{1}$$

where R (mm) is the radius of the planar seed cross-section. The initial contact of seeds is based on the Hertz pressure theory acting on the contact surface $a_S = \sqrt[3]{3\cdot F\cdot(1-\nu_1^2)/E_1 + (1-\nu_2^2)/2/1/2R_1 + 1/2R_2}$, and can be written as $p_S \leq p_{max} = 3F/2\pi\cdot a_S^2$ (Raji & Favier, 2004), where F(N) represents the value of the acting force, ν_i is Poisson's ratio, and E_i (MPa) is the modulus of elasticity in compression.

During seed rearrangement the contact stress is gradually reduced according to the Hertz theory. Normal force F_n can be described by Eq. (2) and then the corresponding normal contact stiffness C_n (Eq. (3)) can be obtained. C_n can be expressed as the elementary increment of the total differential of the normal force dF_n based on the principle of nonlinear compression of a spring, as shown by Raji and Favier (2004).

$$F_n = \psi\cdot\sqrt{\delta^3\left(\frac{R_1R_2}{R_1+R_2}\right)}\cdot\left[\frac{1-\nu_1}{G_1}+\frac{1-\nu_2}{G_2}\right]^{-1}\Bigg|_{T=\text{const}} \tag{2}$$

$$dF_n = C_n\cdot d\delta|_{T=\text{const}} \Rightarrow C_n = \frac{dF_n}{d\delta}\Big|_{T=\text{const}} = \vartheta\cdot C_S^{-1}\cdot\sqrt{\frac{\delta}{R}} \tag{3}$$

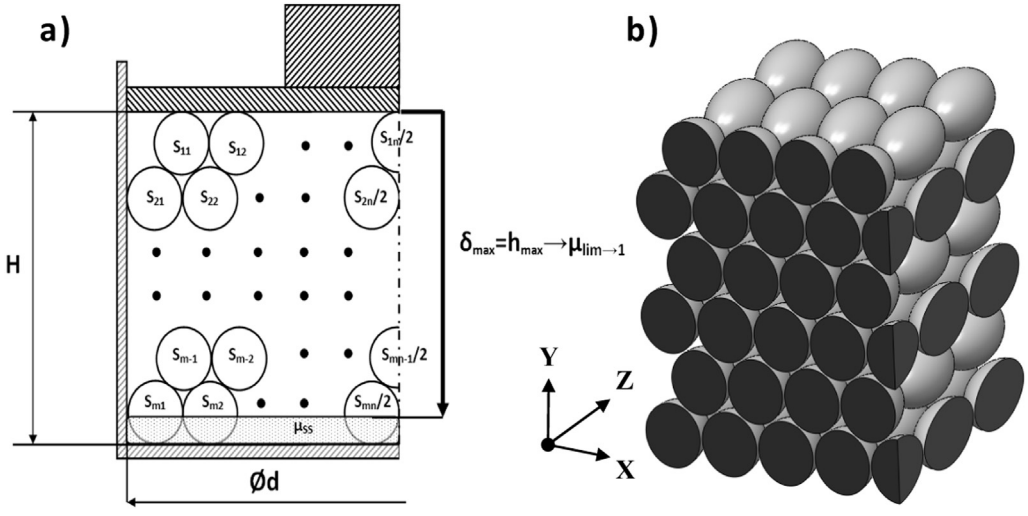

Fig. 1 – Model of ideally ordered bulk seeds of *Jatropha curcas* L.: a) model for mathematical description, b) 3D model.

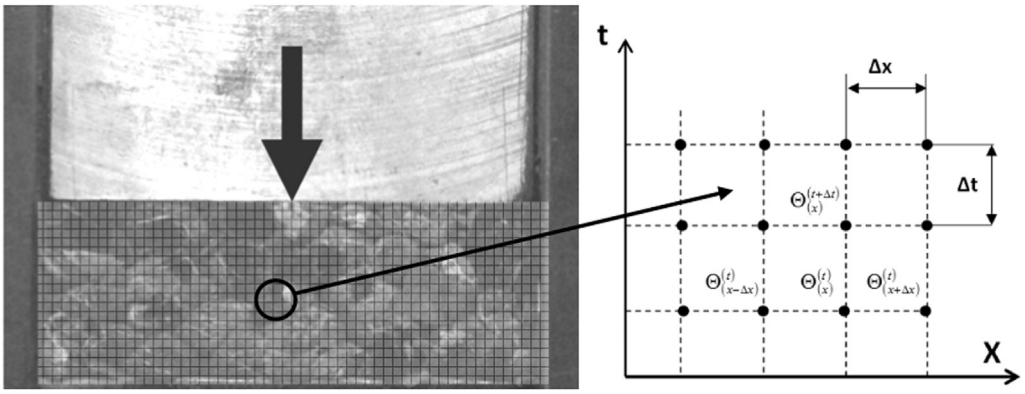

Fig. 2 – Area filled with *Jatropha curcas* L. seed covered by a rectangular mesh (left), mathematical expression of differential calculus (right).

where F_n (N) is normal contact force, δ (mm) is compression value, R_1, R_2 (mm) are radiuses of the surface cross-section of seed 1 and seed 2, between which the contact occurs (in the initial position of ideally arranged seeds it will apply that $R_1 = R_2 = R$), G_i (MPa) is the shear modulus of elasticity, C_n is the normal contact stiffness, C_S (–) is a coefficient of the material structure stiffness, $\sqrt{\delta/R}$ is a dimensional ratio, which can be characterised as the touch contact, and ψ, ϑ are dimensionless constants (Raji & Favier, 2004). The total stress in the structure of the seed increases with the increasing value of volumetric strain because the effect of the increasing force is higher than the effect of the contact coefficient. Therefore, gradual compression leads to uneven strain among the seeds, which will increase the coherence of the seeds in the newly developed compact structure. This mechanical system can be considered as a superstructure. Its increasing specific density is an important factor for the efficiency of the pressing process, affecting the amount of extruded oil. The term superstructure can be explained in the physical nature of a compression system as "seed-oil-air", where the maximum packing density μ_{SS} of the superstructure is a function of deformation $\mu_{SS} = f(\delta)|_{max \to 1, \delta \to H}$, whereby the limit of this function is 1. The mechanical properties of the superstructure are different from the properties of a single seed because the superstructure consists of several phases (gas–liquid–solid) whose ratios during the compression are changing. Initially, air dominates in this structure. With increasing compression the oil and seed mass dominates and in the final compression phase it is only the seed mass. Thus, the stress in the deformed seeds will be a function of the strain of the superstructure $\sigma_{SS} = f(\varepsilon_{SS})|_{> \text{low oiliness point}}$, where ε_{SS} can be suitably determined by the relations of continuum mechanics using the Lagrange or Euler description.

2.3. Description possibilities of strain kinematics

The finite element method was used in this study to describe the kinematics of seed strain. It is well known that the applicability of FEM is significantly influenced by the availability of adequate software and hardware. Therefore, approximate knowledge of the strain and stress distribution in any area of the compressed seed structure can be gained using the numerical method of finite differences. This method is very applicable when the compression process is visualised. Assuming that the strain in a freely selected area of a compressed structure is described with a known function or experimentally measured value and denoted as $\Theta(x, t)$, then a mathematical set of members (Fig. 2) can be built in the field of geometric and time values $0 < x < \phi d$, $t > 0$. The set consists of a square grid of straight lines parallel to the axis t with spacing Δx and straight lines parallel to the axis X with spacing Δt as depicted in Fig. 2. Let $N_{(m)}$ be the mth freely selected point of the grid and $N_{(m+\Delta x)}$, $N_{(m+\Delta t)}$, $N_{(m-\Delta x)}$ be the adjacent points. Then it is possible to assign the parameterised coordinates to individual points using Table 1. If Δx, Δt are sufficiently small then the other members can be disregarded in the Taylor series, as stated in Legras (1956). A differential expression of Eq. (4) can be written for the nodes $N_{(m+\Delta x)}$, $N_{(m-\Delta x)}$. An analytically described change of function $\Theta(x, t)$ according to time t can be expressed through the differential $\Theta_{(x)}^{(t+\Delta t)} - \Theta_{(x)}^{(t)}$ according to Eq. (5). This leads to the energy balance equation and its differential expression according to Eq. (6). The balance equations of the strain can also describe other seemingly different physical problems, for example under pressure in porous granular structures such as soil (Sathar, Worden, Faulkner, & Smalley, 2012; Wang, Zheng, Li, & Ge, 2011).

$$\left.\begin{aligned} \Theta_{(x+\Delta x)}^{(t)} &= \Theta(x+\Delta x, t) = \Theta(x,t) + \Delta x \frac{\partial \Theta}{\partial x}(x,t) + \frac{\Delta x^2}{2}\frac{\partial^2 \Theta}{\partial x^2}(x,t), \\ \Theta_{(x-\Delta x)}^{(t)} &= \Theta(x-\Delta x, t) = \Theta(x,t) - \Delta x \frac{\partial \Theta}{\partial x}(x,t) + \frac{\Delta x^2}{2}\frac{\partial^2 \Theta}{\partial x^2}(x,t) \end{aligned}\right\} \to \frac{\partial^2 \Theta}{\partial x^2} = \frac{\Theta_{(x-\Delta x)}^{(t)} + \Theta_{(x+\Delta x)}^{(t)} - 2\Theta_{(x)}^{(t)}}{\Delta x^2} \quad (4)$$

Table 1 – Coordinates of selected structure points for differential calculations.

Point of grid	Coordinates X	Coordinates t
$N_{(m)}$	x	t
$N_{(m+\Delta x)}$	$x + \Delta x$	t
$N_{(m+\Delta t)}$	x	$t + \Delta t$
$N_{(m-\Delta x)}$	$x - \Delta x$	t

$$\Theta_{(x)}^{(t+\Delta t)} - \Theta_{(x)}^{(t)} = \Theta(x, t+\Delta t) = \Theta(x,t) + \Delta t \frac{\partial \Theta}{\partial t}(x,t) - \Theta(x,t) = \Delta t \frac{\partial \Theta}{\partial t}(x,t) \quad (5)$$

$$\left.\frac{\partial^2 \Theta}{\partial x^2} = \xi \frac{\partial \Theta}{\partial t}\right\} \rightarrow \Theta_{(x+\Delta x)}^{(t)} + \Theta_{(x-\Delta x)}^{(t)} - 2\Theta_{(x)}^{(t)} = \frac{\Delta x^2}{\Delta t} \cdot \xi \cdot \left(\Theta_{(x)}^{(t+\Delta t)} + \Theta_{(x)}^{(t)}\right) \quad (6)$$

$\Theta(x, t)$ is a known or measured value at point $N_{(m)}$, $\Theta_{(x+\Delta x)}^{(t)}$, $\Theta_{(x)}^{(t+\Delta t)}$, $\Theta_{(x-\Delta x)}^{(t)}$ is a differential value of function $\Theta(x, t)$ of an adjacent point at the differential distance $N_{(m+\Delta x)}$, $N_{(m+\Delta t)}$, $N_{(m-\Delta x)}$, ξ is a compression factor depending on the type of compressed seed structure (ripe, unripe, over-ripe), for which it can be suitably chosen that $\xi \cdot \Delta x^2 = 2\Delta t$. Then, the dependence $\Theta_{(m+\Delta t)} = \Theta_{(m+\Delta x)} + \Theta_{(m-\Delta x)}/2$ approximately applies.

It is clear that, through the differential mathematical expression, the stress concentration in the finite part of the selected area can be determined and described as a set of values. The accuracy is affected by the size of the selected rectangular grid. It is also important to prescribe appropriate boundary and initial conditions at the boundaries of this set according to Eq. (7).

$$\left.\begin{array}{l} \Theta(x_{min}, t) = 0 \quad \text{and} \quad \Theta(x_{max}, t) = 0 \\ \frac{\partial \Theta(x_{min}, t)}{\partial t} = 0 \quad \text{and} \quad \Theta(x_{max}, t) = 0 \end{array}\right| \begin{array}{l} t=0, \delta=0 \\ t \neq 0, \delta \rightarrow h_{max} \end{array} \quad (7)$$

2.4. *Compression experiments of J. curcas L. seeds in semi-cylindrical vessels to visualise the complex problem*

Previously (Herak, Kabutey, Divisova, & Simanjuntak, 2013) seed compression experiments were done in whole cylinders of different diameters (Ø60, Ø80 and Ø100 mm). From these experiments Eq. (8) was derived.

$$F_D(x) = A_D\left[\tan(B_D \cdot x)^2\right] \quad (8)$$

Table 2 – Determined coefficients of deformation characteristics for different diameters of pressing vessel for bulk seeds of *Jatropha curcas* L.

Type of cylinder	D (mm)	H (mm)	A_D (N)	B_D (mm^{-1})
Cylinder	60	50	4.527	0.041
	80		5.057	0.041
	100		11.33	0.040
Semi-cylinder	60		2.011	0.031

D – inner diameter of pressing vessel, H – different pressing seed heights, A_D – force coefficient of mechanical behaviour, B_D – deformation coefficient of mechanical behaviour.

where F_D (N) is compressive force, A_D (N) is force coefficient of mechanical behaviour, B_D (mm^{-1}) is deformation coefficient of mechanical behaviour and x (mm) is displacement.

Generally, Eq. (8) is applicable for a description of the mechanical behaviour of compression of *J. curcas* L. seeds in different vessels. This is due to the fact that unknown coefficients A_D and B_D can be derived through the Levenberg–Marquardt algorithm for almost any vessel shape (e.g., a cylinder, semi-cylinder, prismatic vessel, etc.) as shown in Table 2. Therefore for experimental study and visualisation of the strain kinematics of seeds, a semi-cylinder could be used. The compression experiments of *J. curcas* L. seeds were performed in a semi-cylindrical laboratory vessel to obtain a closer understanding of the mutual damage of the seeds in the compression process. This can provide an insight into the actions taking place between the seeds during compression and help visualise the deformation of the seeds in the compression process. It is assumed that the geometry of the compression vessel, the volume of which substantially exceeds the volume of an individual seed ($V_{seed} \ll V_{vessel}$), will not have any significant effect on the actions taking place. It can be expected that the deformation process during the compression of the seeds will be similar throughout the cylinder to the compression of the seeds in a semi-cylinder. The dividing plane of the semi-cylindrical vessel, which is made of glass to aid visualisation, is a technologically modified surface treatment with a friction coefficient of 0.15, i.e. the value of the corresponding friction between the seeds (Karaj & Müller, 2010). The friction coefficient of 0.15 between the seeds was subsequently used in the FEM simulation. The samples of *J. curcas* L. seeds used in these experiments were obtained from North Sumatra, Indonesia. The tested seeds had an almost ellipsoidal shape with mean dimensions of 17 × 10 × 9.3 mm. The characteristic physical properties of the seeds are listed in Table 3. Seed samples were placed similarly to the theoretical ideal arrangement (Fig. 1). Compression was performed in the semi-cylinder with diameter 60 mm. For visualisation of the seed compression strain and the critical damage, a dividing plane in the compression cylinder made of special tempered glass (designed for loads of up to 100 kN) was used. The glass was tightly fixed to the base and walls of the compression cylinder. In the base there were grooves for draining the extruded oil. The maximal displacement of the compression piston was $\delta = 37.5$ mm. Measurements were carried out in the laboratories of the Faculty of Engineering, Czech University of Life Sciences Prague. A diagram of the design and arrangement of the experiment is shown in Fig. 3. The obtained experimental data describing the compression of *J. curcas* L. seeds in the semi-cylinder and cylinders (Herak, Kabutey, Divisova, & Simanjuntak, 2013) will be compared with established FEM models.

2.5. *FEM model description*

2.5.1. *FEM model description*

FEM models were established for the visualisation and study of the mechanical properties of seeds compressed in the cylinders and semi-cylinder. Dimensions of the compressing vessels specified in Table 3 are the same as in the experiments (Herak, Kabutey, Divisova, & Simanjuntak, 2013), where the

Table 3 – Characteristics of the *Jatropha curcas* L. seeds used in the experiment.

Ød (mm)	H (mm)	δ (mm)	V (mm³)	m_s (g)	M_c (% d.b.)	P_f (%)
60	50	37.5	141.390 ± 3.800	54.83 ± 0.74	8.5 ± 0.2	60.02 ± 2.99
80			251.360 ± 13.520	98.35 ± 1.24		59.66 ± 3.45
100			392.750 ± 14.980	156.34 ± 2.29		58.96 ± 3.22

The characteristics in the table are based on the experimental values listed in publications (Herak, Kabutey, Divisova, & Simanjuntak, 2013; Herak, Kabutey, & Hrabe, 2013), where m_s is the mass of a seed, M_c (%) is moisture content, and P_f (%) is porosity of the seeds calculated from the relationship $P_f = (1 - \rho_b/\rho_t)\cdot 100$ (Blahovec, 2008), where ρ_b is volume density and ρ_t is specific density.

pressing cylinders and the piston had diameters of 60, 80 and 100 mm and the model of semi-cylinder had a diameter of 60 mm.

The models were assembled to provide an approximate solution and study the complex issue of the deformation of seeds compressed in a cylinder. Since these are 2D FEM models, it was necessary to select the appropriate cutting plane of the seed system because the seeds have multiple axes of symmetry. It was possible to perform the cutting plane on the X–Y or Y–Z plane (Fig. 1). In the first case, the cutting plane is circular and in the second it is elliptical. Considering the fact that the previous results (Petrů, Novák, Herák, & Simanjuntak, 2012) from the 3D seed model showed that there was less stress and strain on the Y–Z plane, a model assembled with a cutting plane on the Y–Z plane would not be appropriate for the study of the limit states of stress and strain in the seeds. Therefore, a circular cutting plane was selected, i.e. on the X–Y plane (Fig. 1). It is clear that this simplification leads to a certain discrepancy in the results compared with the real experiments; however, the obtained information will be valuable for an initial understanding of the complex phenomena which take place during compression of the *J. curcas* L. seeds. A 3D FEM simulation will be assembled in future work to provide a comprehensive study and extension of the knowledge obtained from the 2D FEM models. The assembled FEM models describe isothermal compression under laboratory conditions (22 °C). In reality this process is exothermic, whereby the temperature of the system increases with increasing compression. This causes a decrease in viscosity, which improves the oil extrusion. The model of the cylinder and semi-cylinder is regularly filled with models of *J. curcas* L. seeds with idealised geometry. Mechanical properties were considered for the mature seeds, which were used in the experiments. The seeds have an identical initial geometry $\Omega_{ripe}|_{t=0}$ and a regular ideal arrangement, which creates a so-called triangular arrangement in the cross-section as in Fig. 1. Individual seeds of the same ripeness exhibit different levels of stress and strain at time $t \neq 0|_{\delta \neq 0}$ during compression. This is due to the fact that the geometry of the seeds is a function not only of strain $\varepsilon_S|_{T=const}$ and value of compression δ but also the compressibility function ψ, which is different from the compressibility of a single seed. A single compressed seed is damaged due to the internal stress (Petrů, Novák, Herák, & Simanjuntak, 2012) but during compression of several (bulk) seeds the mutual contacts cause an increase in system coherence (the seeds have less space for expansion). This leads to an increase in contact pressure p_S, which causes a different mutual strain of the seeds. The different strain is caused due to inhomogeneous seed rearrangement, unlike the initial point contact at time $t = 0|_{\delta=0}$. The resulting reorganisation and uneven seed deformation cause the formation of stress concentrators on the outer boundary of the seeds that causes the initial crack growth (Fig. 4). Based on the geometric dimensions of real samples of *J. curcas* L. seeds, a 3D model of a rotating ellipsoid with characteristic dimensions of 17 × 10 mm (volume V = 885.91 mm³) was created, wherein one seed in the cross-section has a diameter of 10 mm (S = 78.53 mm²). Geometric models were created by the use of

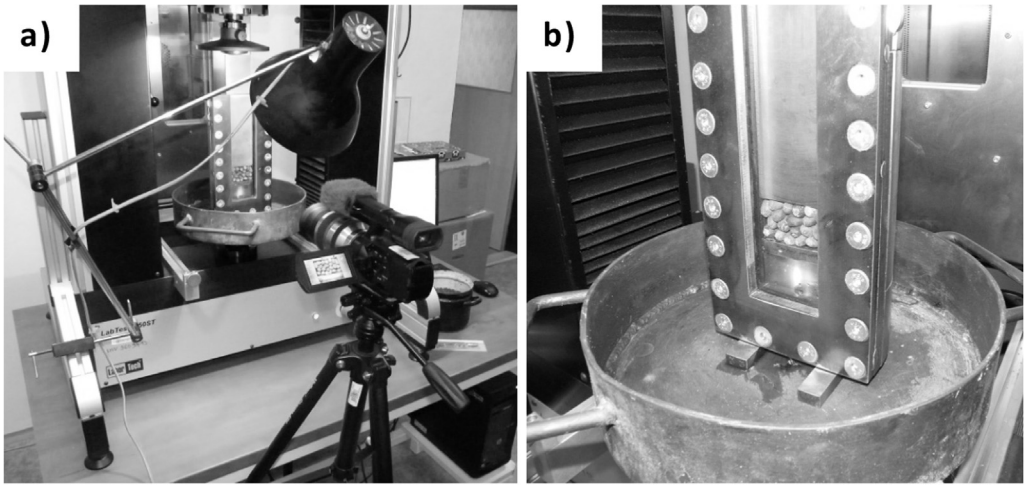

Fig. 3 – Experiment for the visualisation and study of seed deformation during compression: a) experimental arrangement, b) detail: semicircular compression cylinder with piston filled with seeds.

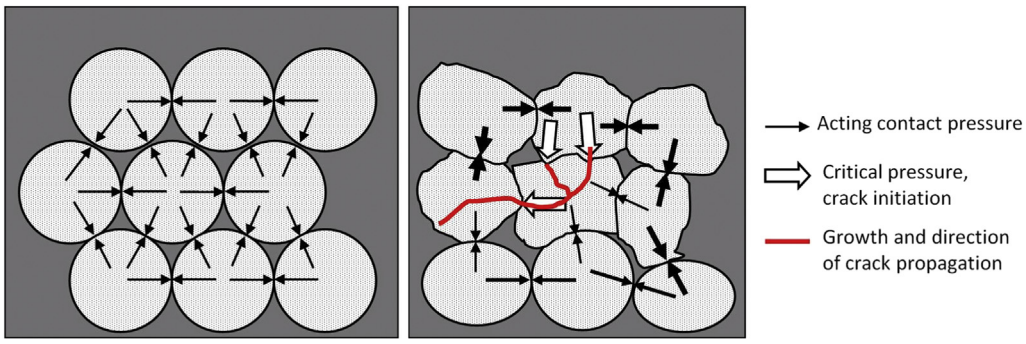

Fig. 4 – Settlement and seed reorganisation of *Jatropha curcas* L. during compression: initial configuration with point contact pressure at $t = 0$, $\delta = 0$, $p_s \rightarrow p_{smin}$ (left), strain of seeds under uneven contact pressure leading to crack initiation at $t \neq 0$, $\delta \neq 0$, $p_s \rightarrow p_{scrit}$ (right).

Table 4 – Data required for the FEM model.

Model	Area S (mm^2)	Density ρ (kg m^{-3})	Low oil point (–)	Initial modulus E (MPa)	Initial bulk modulus K (MPa)	Initial shear modulus G (MPa)
Ripe seed	170	971	0.4	3	2.174	0.974
Pressing plunger & cylinder	2827.4 (Ø60) 5026.5 (Ø80) 7853.9 (Ø100)	7850	–	210 000	–	65.625

Initial modulus and low oil point are taken from (Herak, Gurdil, Sedlacek, Dajbych, & Simanjuntak, 2010; Herak, Kabutey, Divisova, & Simanjuntak, 2013; Herak, Kabutey, & Hrabe, 2013), initial bulk and shear modulus are calculated from Eq. $K = E/3 - 6\mu_S$ and $G = E/2 + 2\mu_S$.

the parametric CAD software (Computer Aided Design) SolidWorks 2012 (Dassault Systèmes SolidWorks Corporation, Waltham, MA, USA). The finite element mesh for each submodel of the seeds, the compression piston and the cylinder were made using the special software Altair HyperMesh 11 (Altair Engineering, Inc, Nagog Park, MA, USA). In order to achieve a sufficiently planar mesh, quadrilateral elements (Quads) for the seeds were designed with an average size of 0.5 mm. The individual parameters applied in the FEM model are shown in Table 4, where the material properties are based on the FEM model of mature *J. curcas* L. seeds (Petrů, Novák, Herák, & Simanjuntak, 2012). The FEM software PAM CRASH (ESI Group, Paris, France) with an explicit algorithm was used for the model analysis. The cylinders and compression pistons of the given dimensions formed the boundaries of contact with the seeds and were considered to be rigid bodies, which are generally described as $\sigma_{PP,C} \leq 0$, $\varepsilon_{PP,C} \leq 0$, $\sigma_{PP,C} \cdot \varepsilon_{PP,C} = 0$. The piston and cylinder are formed from square surface elements with a constant size of 2 mm for the piston and 3 mm for the cylinder. The number of elements of the model is shown in Table 5. The boundary and initial conditions of the FEM models of compressed seeds are shown in Fig. 5 and they are the same as in the real experiment. The lower base of the cylinder was firmly secured against displacement and rotation in all directions, $U_i = R_i = 0$, where $i = X, Y, Z$ and piston had the same boundary conditions, and the only displacement in the vertical direction is $U_Y \neq 0$. The velocity of the piston was 1 mm s^{-1}. The *J. curcas* L. seeds were allowed displacement and rotation in all directions $U_i = R_i \neq 0$. The thickness of the contact between the seeds and the

Table 5 – Parameters characterising the properties of the FEM model.

Part	Size of element (mm)	Number of elements (–)	Friction coefficient between the parts (–)	Thickness of contacts (mm)	Time step Min (s)
Pressing plunger	2	225 (Ø60) 300 (Ø80) 375 (Ø100)	0.1	0.05	$6.797 \cdot 10^{-5}$
Ripe seed	0.5	13 380 (Ø60) 18 120 (Ø80) 22 860 (Ø100)	0.15		$2.223 \cdot 10^{-7}$
Cylinder	3	200 (Ø60) 220 (Ø80) 235 (Ø100)	0.1		$3.267 \cdot 10^{-4}$

Friction coefficients were taken from Karaj and Müller (2010) and were reduced from 0.22 to 0.1 due to the presence of pressed oil, which acts as a lubricant.

surface of the piston and the cylinder was set at 0.05 mm. The coefficient of friction between the seeds and the surface of the cylinder and piston is shown in Table 5. The value of the friction coefficient is very important for the mutual contact. The most important factor for modelling both the compression of the bulk seeds and compression of a single seed is the development of initial contacts on the surfaces of the individual piston–cylinder–seed parts of the model. At the beginning of the pressing process the contact surface a_S is described by Hertz pressure. This area gradually increases as shown in Fig. 6. The FEM model of compressed seeds places high demands on computing time due to the complicated contact conditions and material and geometric nonlinearity. In order to correctly create the contacts, it is necessary to ensure that the change in the normal contact force ΔF_n between two or more contact pairs does not exceed the critical value of the normal contact stiffness C_n^{crit} (Eq. (9)). Changes in the normal contact force ΔF_n that lead to instability and divergence in the calculation may be due to inappropriate boundary conditions on the boundary of the contacts. This usually leads to the penetration of elements and objects (Fig. 7a), if the critical value of the contact stiffness on the Master and Slave element nodes representing the seed contacts is exceeded (Fig. 7b). This leads to divergence and subsequent calculation error. The problem is in the concept of Dirichlet boundary conditions describing the outer boundary (type of specified boundary condition) and the inner boundary (among the structures of the seeds for the formation and

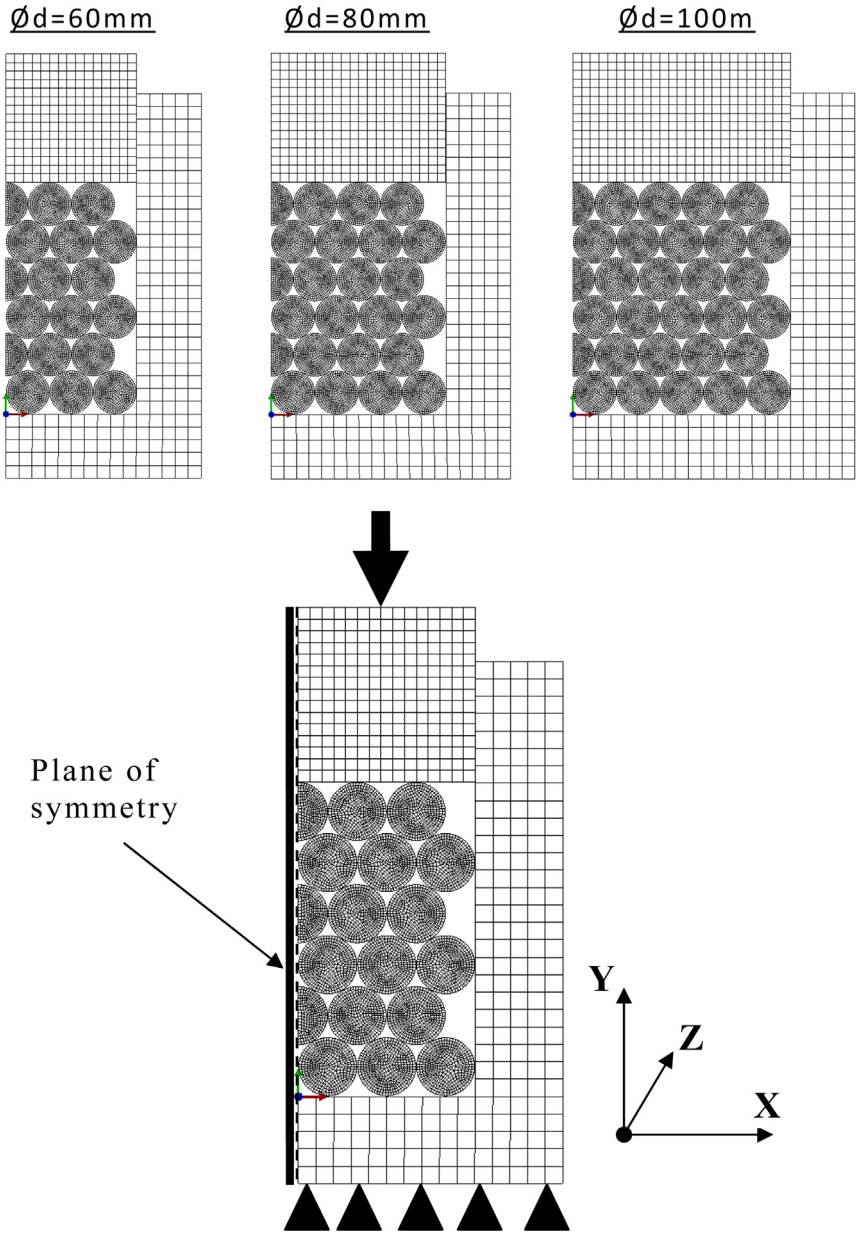

Fig. 5 – FEM models of individual compression cylinders with *Jatropha curcas* L. seeds (above), initial boundary conditions of the FEM models (below). $U_i = 0$ fixed elements against movement in X, Y, Z direction (cylinder); $R_i = 0$ fixed elements against rotation in X, Y, Z direction (cylinder); $U_y \neq 0$ non-fixed elements for movement in Y direction (pressing plunger); $v_y = 1$ mm s^{-1} is velocity in direction Y (pressing plunger).

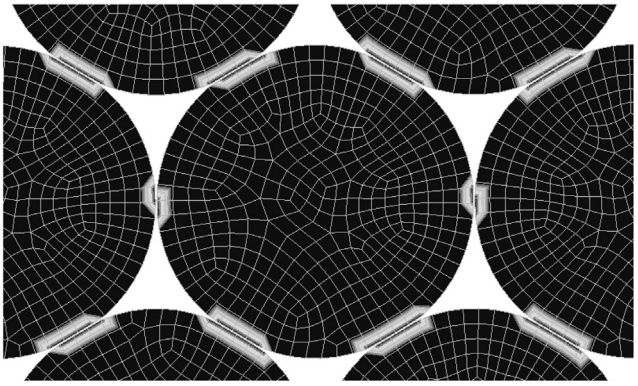

Fig. 6 – FEM model: contact area a_S of the seeds on their outer boundary.

propagation of cracks). It is necessary to define the corresponding parameters of contacts (Fig. 7c) that allow a sufficiently long period of time to maintain the stability of the calculation. This can be achieved by forced restrictive conditions for optimisation of a minimum through Kuhn–Tucker condition (Birbil, Frenk, & Still, 2007). This is given by Eq. (10). The discrete formulation of contact boundary conditions must be done in such a way that the contact is created in pairs of opposite nodes of the finite element mesh, where each of the nodes constituting the pair belongs to an opposite body. The normal vectors $n^{(i)}$ and $n^{(j)}$ are prescribed for each contact pair. If the condition is $n^{(i)} + n^{(j)} = 0$ then it prevents the penetration of the elements. Conditions defined in this way lead to a solution, which will prevent penetration of bodies before the occurrence of critical damage.

$$\Delta F_n = C_n^{crit} \cdot \Delta n_E \tag{9}$$

$$\nabla F_n(\delta, t) + \sum_{i=1}^{m} \sum_{j=1}^{l} \left(k_i \cdot \nabla \Lambda_i(\delta, t) + l_j \cdot \nabla \Gamma_j(\delta, t)\right) = 0 \tag{10}$$

where ΔF_n (N) is a change in normal contact forces, C_n^{crit} is the critical value of the normal contact stiffness, Δn_E is a change in the fractional size of the overlap elements, which is transferred by nodes. $\Lambda_i \leq 0$ for $i = 1, 2, \ldots, m$ are restrictive conditions for inequality, $\Gamma_j = 0$ for $j = 1, 2, \ldots, l$ are restrictive conditions for equality, k_i, l_j for $i, j = 1, 2, \ldots, m$ are contacts which meet the condition of regularity, and ∇ is the divergence operator.

The actual change in the difference of mutual seed overlap Δn_E in the contact area is directly proportional to the speed of movement of the seeds v_S for a given time $\Delta n = v_S \cdot \Delta t$. The change of contact forces in a tangential direction can be obtained analogously from the equation $\Delta F_T \leq \Delta F_N \tan \phi + c$, where c is the value of viscosity of contact for achieving a plastic deformation of the contact. The total strain and crack propagation has a dynamic character, where an expression of the speed of seed movement v_S may be based on basic relation of Newton's second law Eq. (11).

$$\sum m_{Si} \cdot \frac{\Delta v_S}{\Delta t} = \sum F_i \rightarrow \Delta v_S = \frac{\sum F_i}{\sum m_{Si}} \Delta t \tag{11}$$

where $\sum F_i$ (N) is the sum of normal and tangential forces acting on the contact, $\sum m_{Si}$ is the sum of the seed mass, and Δv_S is a change in the speed of seed movement.

The right choice of time step Δt has been shown in numerous studies to also be an important factor for the calculation. Hedjazia, Martin, Guessasma, Della Valle, and Dendievel (2012) studied the crack propagation in the material of a vitreous biopolymer through DEM and FEM and reported that the results of DEM show higher sensitivity of the calculation to a longer time step in comparison with FEM. The time step size Δt is affected by the final size of the smallest element, which occurs due to the fracture toughness. Zeng and Grigg (2006) state that for modelling strongly nonlinearly ground material (rock mass), FEM can be used to describe its softening. The results are closer to reality compared to the theory of plasticity but the calculation step is very long. The softening and hardening of the structure of *J. curcas* L. seeds during compression significantly affects the final calculation step. This is due to Von Mises plasticity $F(\sigma)$, which can be applied to Perzyn's rheological model. The critical time step of

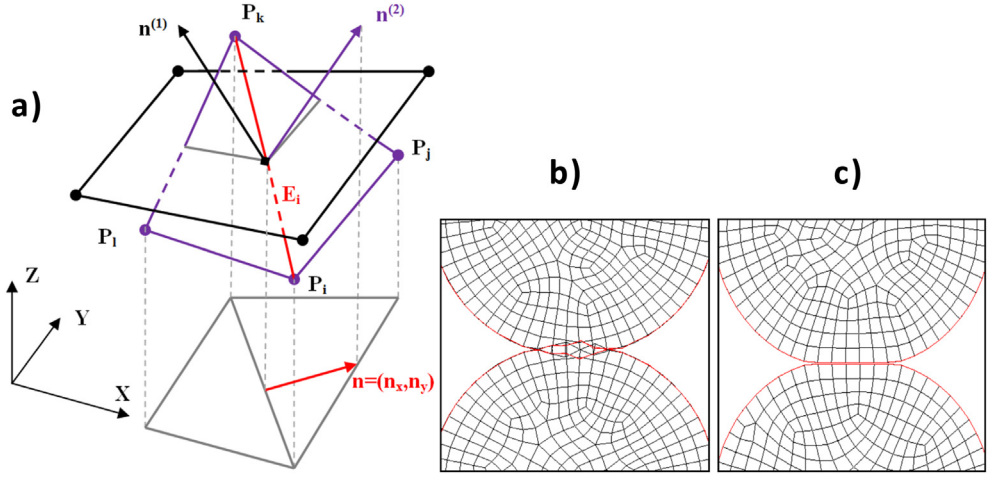

Fig. 7 – a) Diagram of element penetration when the critical value of the normal contact stiffness is exceeded, b) interpenetration of the Master and Slave elements of the individual seeds in contact, c) correctly created contact between the seeds.

the calculation Δt^{crit} is mainly influenced by the smallest element size (Petrů, Novák, Herák, & Simanjuntak, 2012). The use of an explicit algorithm in the finite element method can significantly save on computing time and ensure sufficient stability of the calculation during critical damage of the structure (Harewood & McHugh, 2007; Metzgera, Jarrett, & Dantziga, 2001, Samonds, Morgan, & Lewis, 1985, Zhong, 1993).

3. Results and discussion

Experiments and 2D FEM simulations of the compression of ideally ordered ripe bulk seeds of *J. curcas* L. in cylinders with diameters of 60, 80 and 100 mm and semi-cylinder of diameter 60 mm at a deformation of 75% (displacement of 37.5 mm) were performed. A comparison of seed strain visualisation in a semi-cylinder of diameter 60 mm and FEM models of seed compression in semi-cylinder and the cylinders is shown in Fig. 8. From the visualisation results it is clear that the seed strain during compression in real pressing is very similar to the results of FEM simulation of the pressing in the semi-cylinder. Places where strain in the semi-cylinder achieved a critical value are indicated in Fig. 8b and c. But it is evident that results of FEM simulation of seed compression carried out for semi-cylinder and cylinder models with diameters of 60 mm are not same in different stages of the seed deformation (Fig. 8b, c). This may be due to differences in the spatial arrangement or size of the contact area of the system seed/cylinder. The course of the compressed experimental samples of bulk seeds showed significant anisotropic behaviour influenced by plastic deformation that was manifested as initial crack formation when exceeding the critical stress. If visualisation of the results of the compressing experiment in semi-cylinder is in good agreement with the results of FEM simulation in semi-cylinder, then it can be assumed that the results of FEM simulation of seed compression in the cylinder are meaningful. Because the semi-cylinder geometry is not the appropriate shape for real pressing devices, further results are shown only for the cylindrical geometry. Results of FEM simulations of compression in cylinders (Fig. 9) show the distribution of the equivalent Von Mises stress during volumetric deformation of 20, 40 and 75% at the time 10, 20 and 37.5 s. The distribution of Von Mises stress shows that its growth affects the transfer of contact pressure among the interacting seeds. The strain in the upper row of seeds increases from the axis of symmetry of the cylinder towards the walls of the cylinder and this was observed for all of the diameters of the cylinders. The stress during linear compression of *Jatropha* bulk seeds

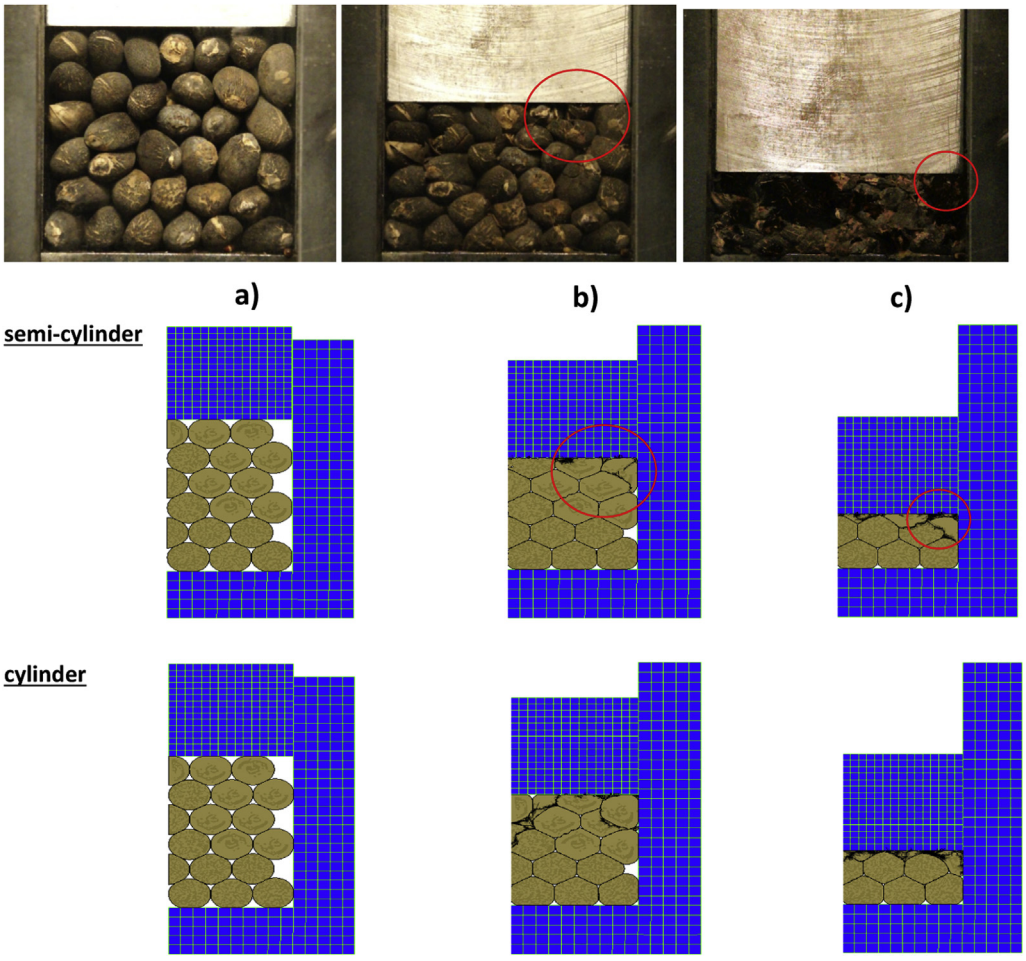

Fig. 8 – Comparison and visualisation of the experiment (Ø60 mm semi-cylinder) and the FEM model (Ø60 mm semi-cylinder and Ø60 mm cylinder) at different stages of seed deformation: a) volumetric strain = 10%, t = 5 s, b) 40%, t = 20 sand c) 75%, t = 37.5 s.

was not homogeneous, which affects the energy efficiency of the pressing process. Deformed seeds are at first critically damaged in contact with the cylinder. This is probably due to the impossibility of the seed mass expanding into the solid cylinder wall. Therefore, the energy required for compressing the bulk seeds was different in various parts of the cylinder. When the volume strain is 20% ($\delta = 10$ mm) it is evident that the seeds in the cylinder with a diameter of Ø60 mm were not critically damaged, while there was damage to the seeds in the cylinders with a diameter of Ø80 mm and Ø100 mm (Fig. 9). This leads us to the conclusion that the seeds placed in the cylinder of a smaller diameter initially have a higher resistance to compression, which is accompanied by a smaller compressibility and greater rigidity – at 40% compression, the stress is about 1.5 times higher than stress in seeds compressed in the larger cylinders. The stress from a damaged seed is transferred to the other seeds, which will also become damaged (Fig. 10). The forces acting on the boundary of the seeds are different. Hence, it can be hypothesised that the bulk seeds are damaged due to internal stress as a consequence of external pressure. From the graph of energy versus strain it follows that the highest initial compressibility of the seeds is in the cylinder with a diameter of Ø100 mm and the seeds in the cylinder with a diameter of Ø60 mm show the lowest compressibility (Fig. 11). This is probably due to the fact that the seeds placed in the cylinder with a larger volume have a greater possibility of motion and reorganisation in the initial stages of compression. At higher degree of volumetric strain, the compressibility of the seeds in the individual cylinders is similar and gradually approaches

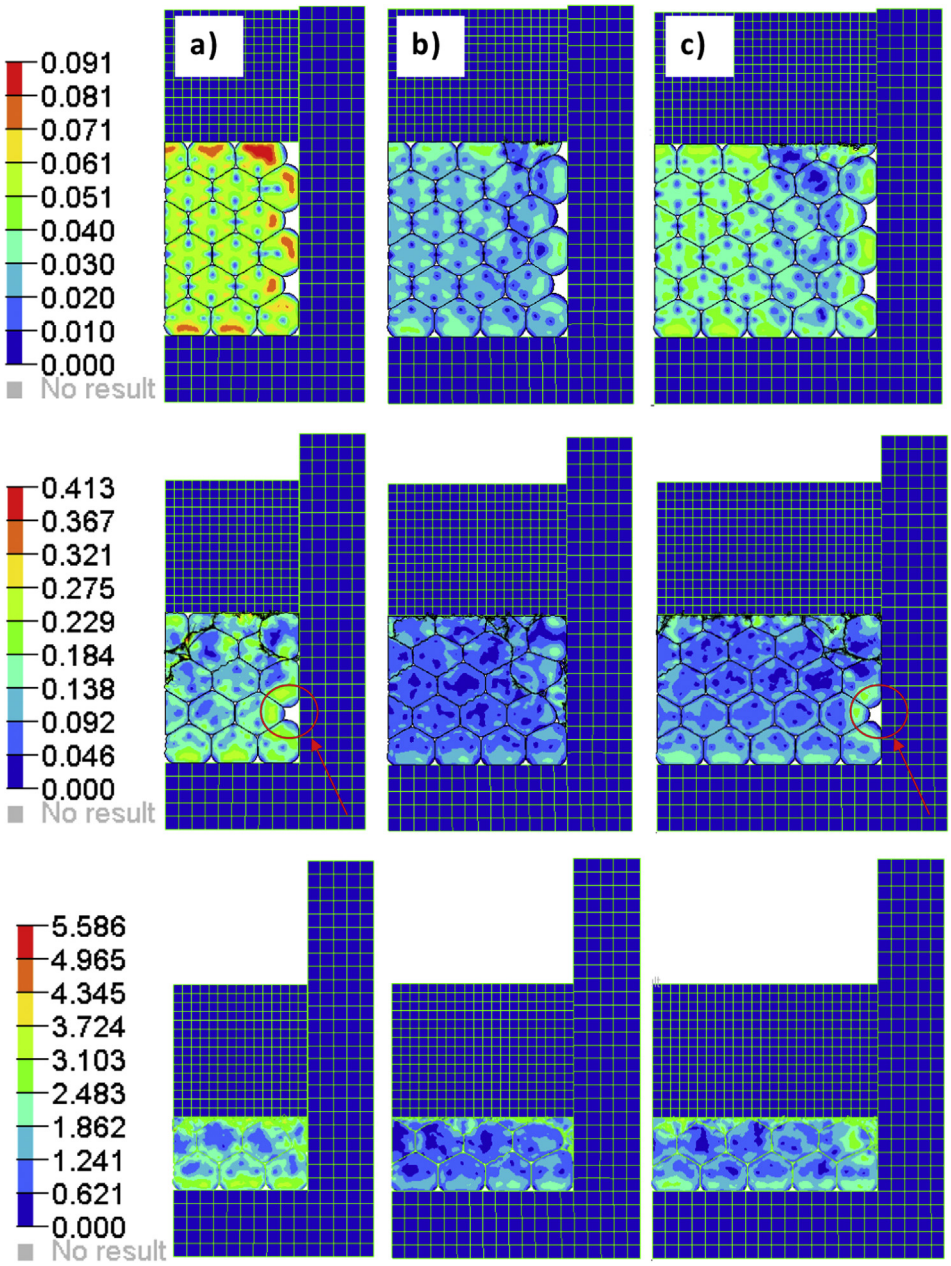

Fig. 9 – Dependence of Von Mises stress [MPa] on the compression: FEM models of compressed *Jatropha curcas* L. seeds at 20, 40, and 75% volumetric strain in cylinders with diameters of a) 60 mm, b) 80 mm, c) 100 mm.

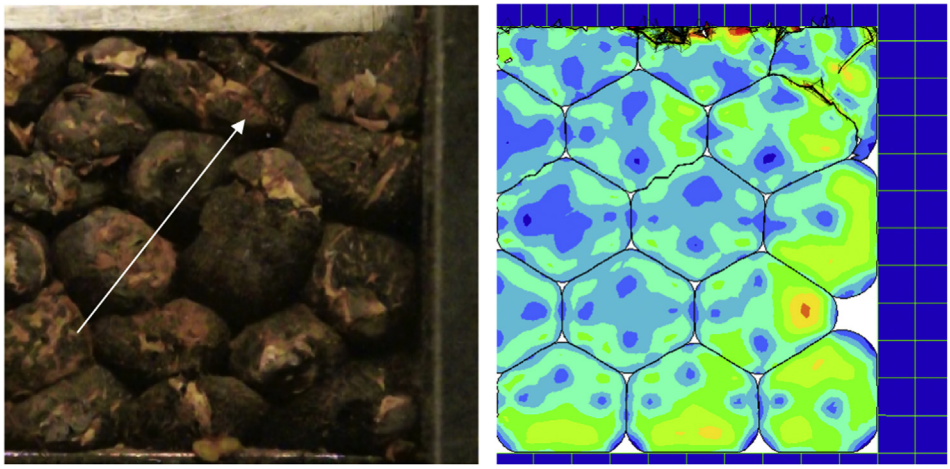

Fig. 10 – Bulk seed compression in semi-cylindrical container: initiation of seed crushing in the real and virtual model of *Jatropha curcas* L. seeds (semi-cylinder) at 40% volumetric strain ($t = 20$ s).

the compression limit, which corresponds to the theory of superstructure incompressibility and also to the law of mass conservation (Fig. 12). The stress and strain energy increase in the order of 60, 100, 80 mm, which does not correspond to the order of the achieved forces shown in Fig. 13. It is important to explain the nature of the problem, which is that the stress and compression energy are related to the area of the piston. This, however, increases quadratically with the given diameter of the piston, which for a diameter of 60, 80, 100 mm affects the resulting courses of compression energy and stress, even though the force for the diameter of 60 mm is marginally less than for the diameter of 80 mm and only slightly less than for the diameter of 100 mm. The obtained results are shown in Table 6. From this it can be hypothesised that seeds placed in a cylinder of smaller diameter are in contact with the cylinder more than seeds are in mutual contact. It is obvious that, in a smaller cylinder, bulk seeds have a higher possibility of moving along the walls due to lower seed/wall friction. Therefore, the seeds take up a new position without their critical strain. It is clear that the coefficient of friction among the seeds and the wall has a significant influence on the optimisation of the design of pressing equipment.

It must be noted, however, that the resulting order of 60, 100 and 80 mm (Fig. 12) can also be given by the immediate arrangement and reorganisation of the seeds in each cylinder. This is visible from the 2D FEM model in Fig. 9, where a gap (red arrow) is visible for the 40% deformation in the case of cylinders with Ø60 and Ø100 mm and the seed compression system has a greater immediate surface packing density, whereas in the Ø80 mm cylinder there is no free space, so its surface packing density is less. It is important to study and refine these results further using 3D FEM models. This would provide information which would confirm or disprove whether the results of the 2D model are transferable and could be applied to a real system of compressed *J. curcas* L seeds. Figure 13 shows a comparison of the force depending on the strain obtained from the experiment made in cylinders and semi-cylinders with the FEM model. The computational deviation of the model was 9%. The results were statistically tested using analysis of variance (ANOVA) and compared with the experimental data fitted by tangent curve (Herak, Kabutey, Divisova, & Simanjuntak, 2013). In Table 7, *P*-values are shown to be between 0.733 and 0.864. The results of the statistical analysis suggest that the finite element method can be used to describe the pressing of *J. curcas* L. bulk seeds. From the obtained results, it can be observed that lower energy intensity of the pressing process can be achieved by reducing the seed/vessel friction with the help of an appropriate structure and treatment of the material. Fomin (1978) showed that the strain energy required for the deformation of a single seed is greater compared to the pressing of bulk seeds. This is given by dynamic effects acting on the seeds (Addy, Whitney, & Chen, 1975). Also, the gradual deformation of bulk seeds and the friction coefficient among the seeds play an important role. These factors can be described with a pressure gradient. If some of the seeds burst, then the stress accumulated in these seeds is transmitted to the other seeds (Blahovec & Řezníček, 1980). The pressure gradient significantly affects the mechanical behaviour of the bulk seeds during the pressing process (Herak, Kabutey, & Hrabe, 2013; Herak, Kabutey, Sedlacek, Gurdil, 2012).

4. Conclusion

Assessment of the energy efficiency of the pressing process of *J. curcas* L. bulk seeds can be improved by 2D FEM simulation and also visualisation of the processes occurring during pressing. Experimental study and visualisation of the mechanical properties of ripe bulk seeds of *J. curcas* L. was done in a semi-cylinder, which allowed observation of the pressing process during all of its stages i.e. from the formation of contacts, through the deformation of seeds, to damage and extrusion of the oil component. This allows a comparison between experimental data and an FEM model describing the mechanical properties of the inhomogeneous anisotropic system of pressed bulk seeds. The assembly of the FEM model can be assessed not only by comparison with the time courses of total compression forces determined experimentally but also by visual comparison of seed deformation inside the

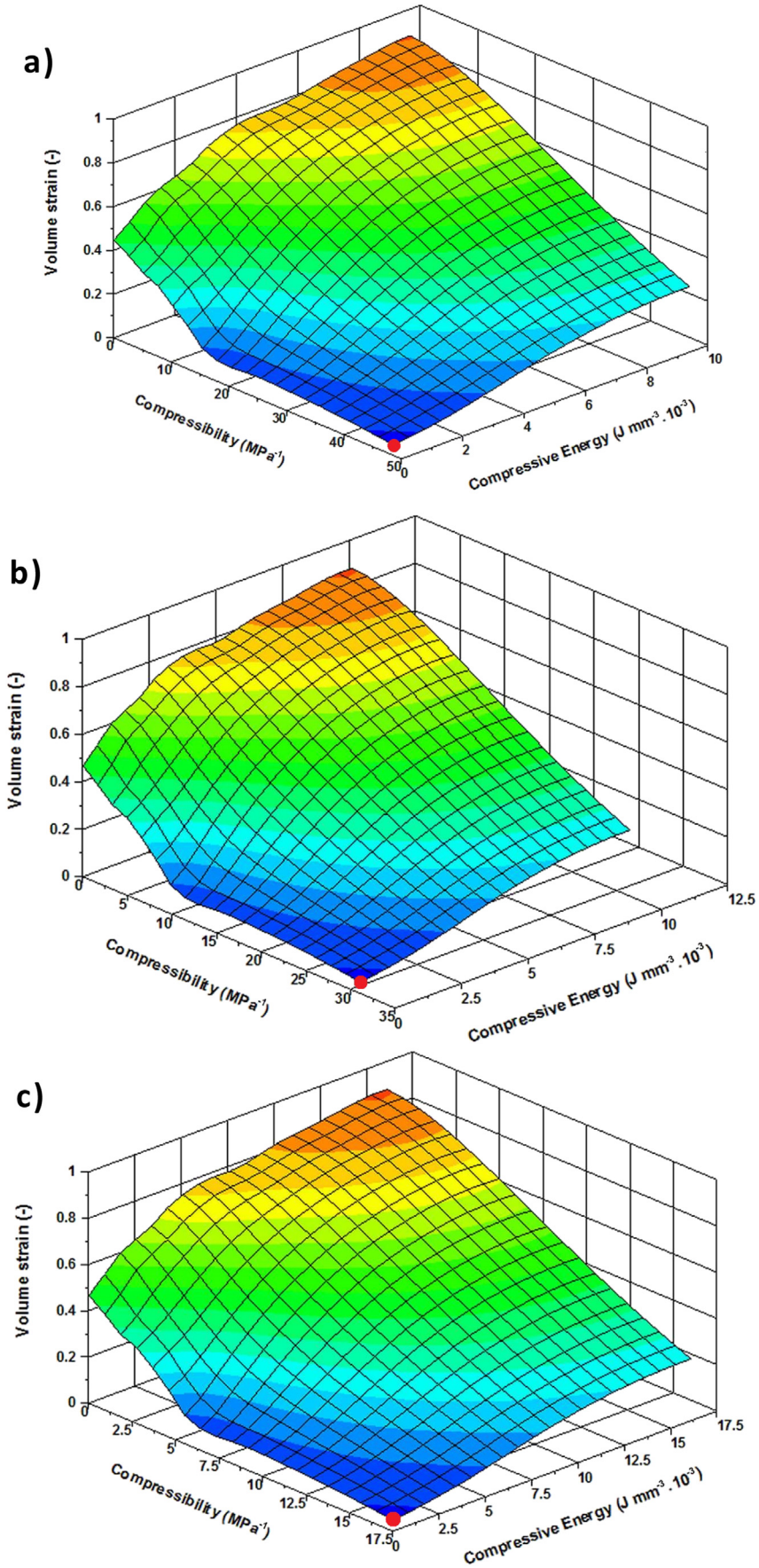

Fig. 11 – Dependence of the compressibility and the energy during seed compression in cylinders with a diameter of a) 100, b) 80, and c) 60 mm; red points indicate the initial compressibility.

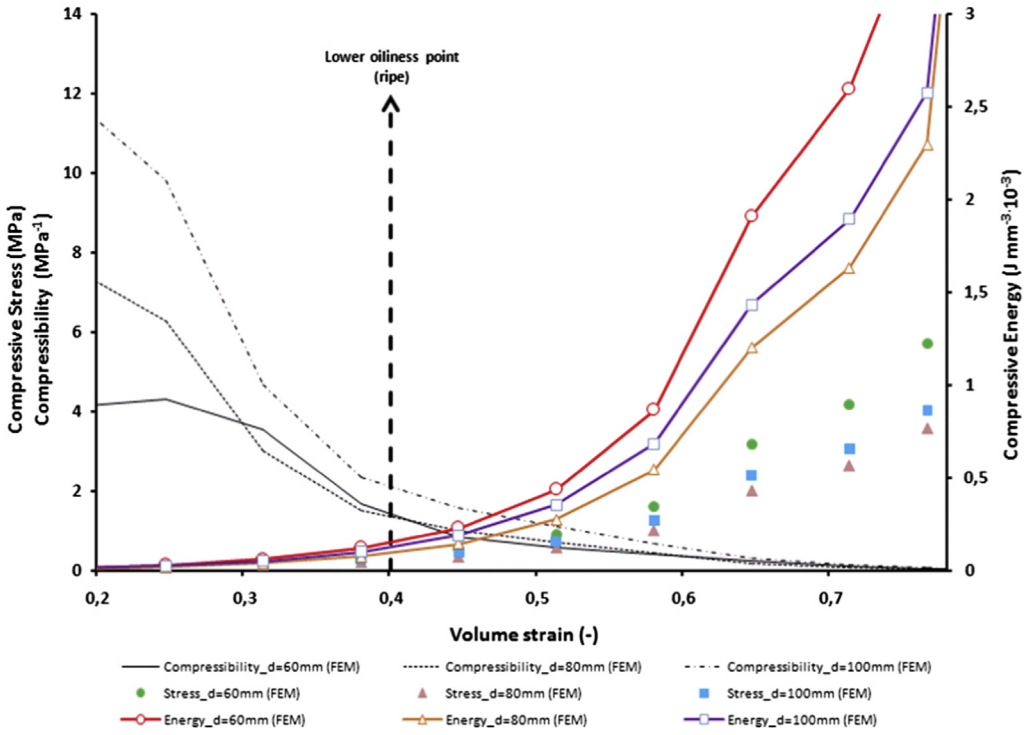

Fig. 12 – Course of compressive stress, compressive energy and compressibility in cylinders with a diameter of Ø60, Ø80, and Ø100 mm in the FEM model of *Jatropha curcas* L. seeds.

device. This makes it possible to find the unknown parameters corresponding to the real pressing process and thus to be able to use the obtained results for an assessment of the energy efficiency of the pressing process. The results of the FEM model showed that a significant role in the initial stages of the pressing process is played by the values of the contact friction in the seed/seed and seed/vessel system. Above all, the value of the seed/vessel friction coefficient has a great importance to the ability of the whole seed formation to reorganise and take a new position, which leads to lower surface porosity in the compressed seed system, whereby the force required for this purpose, and hence the energy, is lower. In addition, it was determined that the emerging superstructure produced from the pressed seeds exists simultaneously in several phases. From the observations of the compression and deformation of the seeds in the cylinder, it is evident that at the same time there are areas with high porosity filled with air, areas approaching the critical strain, areas where the oil is being

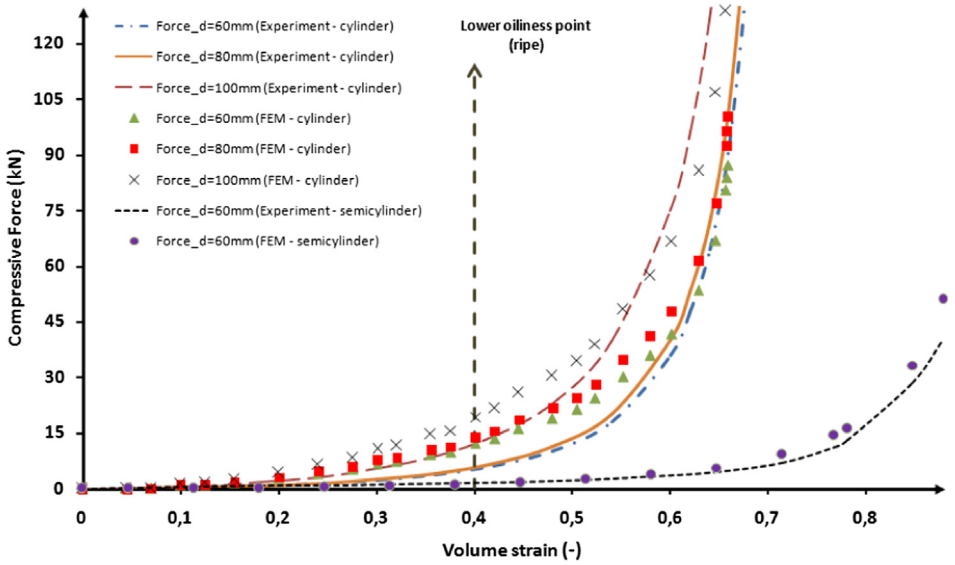

Fig. 13 – Comparison of experiment and the FEM model of *Jatropha curcas* L. seeds for compressive force.

Table 6 – Summary of output data obtained from the FEM model.

Piston and cylinder diameter [mm]	Compression in low oil point (40% of volume strain)			Compression at 75% of volumetric strain		
	Von Mises stress σ_e (MPa)	Compressibility ψ (MPa^{-1})	Volume energy W(ε) (J mm^{-3} 10^{-3})	Von Mises stress σ_e (MPa)	Compressibility ψ (MPa^{-1})	Volume energy W(ε) (J mm^{-3} 10^{-3})
Ø60	0.413	0.931	0.198	5.586	0.0464	3.655
Ø80	0.263	1.418	0.085	3.574	0.0825	2.296
Ø100	0.282	2.469	0.129	4.233	0.129	2.577

Von Mises stress, compressibility and volume energy are compared with the FEM results based on Eq. $\sigma_e = \sqrt{1/2[(\sigma_1-\sigma_2)^2+(\sigma_1-\sigma_3)^2+(\sigma_2-\sigma_3)^2]}$ (Petrů, Novák, Herák, & Simanjuntak, 2012), $\psi = -\gamma\cdot\Delta C$ (Raji & Favier, 2004) and $W(\varepsilon) = [C/2\cdot D\cdot\ln[1+(\tan(D\cdot\varepsilon))^2]]_{\varepsilon_1}^{\varepsilon_2}$ (Herak, Gurdil, Sedlacek, Dajbych, & Simanjuntak, 2010).

Table 7 – Statistical analysis of the FEM model and the experimental data.

Type of cylinder	Piston	F_{rat} (–)	P_{value} (–)	F_{crit} (–)
Cylinder	Ø60	0.0803	0.778	4.255
	Ø80	0.118	0.733	
	Ø100	0.029	0.864	
Semi-cylinder	Ø60	0.105	0.753	4.170

F_{rat} – value of the F test.
F_{crit} – critical value comparing a pair of models.
P_{value} – significance level at which the hypothesis of equality of the models can be rejected.

extruded and areas where the oil is already almost entirely extruded. The 2D FEM models described in this study should provide the basis for the development of further 3D FEM models which can describe the nonlinear mechanical behaviour of oilseeds involving the use of screw extruders or presses and thus to design suitable pressing equipment for processing *J. curcas* L. seeds with minimum energy performance.

Acknowledgements

The results of this project No. LO1201 were obtained through the financial support of the Ministry of Education, Youth and Sports, Czech Republic in the framework of the targeted support of the "National Programme for Sustainability I", the OPR&DI project Centre for Nanomaterials, Advanced Technologies and Innovation No. CZ.1.05/2.1.00/01.0005, the project "Development of Research Teams of R&D Projects at the Technical University of Liberec" No. CZ.1.07/2.3.00/30.0024 and the CREATex project (No. CZ.1.07/2.2.00/28.0321), which was financed by the European Social Fund and the Ministry of Education, Youth and Sports, Czech Republic. This work was supported by the ESF operational programme "Education for Competitiveness" in the Czech Republic in the framework of the project "Support of engineering of excellent research and development teams at the Technical University of Liberec" No. CZ.1.07/2.3.00/30.0065.

REFERENCES

Addy, T. O., Whitney, L. F., & Chen, C. S. (1975). *Mechanical parameters in leaf cell membrane rupture for protein production*. St. Joseph, ASAE paper no. 75-1057.

Adeeko, K. A., & Ajibola, O. O. (1990). Processing factors affecting yield and quality of mechanically expressed groundnut oil. *Journal of Agricultural Engineering Research, 45*, 31–43.

Akinosho, R., Raji, A. O., & Igbeka, J. C. (2009). Effects of compressive stress, feeding rate and speed of rotation on palm kernel oil yield. *Journal of Food Engineering, 93*, 427–430.

Bardet, J. P., & Proubet, J. (1991). A numerical investigation of the structure of persistent shear bands in granular media. *Geotechnique, 41*, 599–613.

Birbil, S. I., Frenk, J. B. G., & Still, G. J. (2007). An elementary proof of the Fritz–John and Karush–Kuhn–Tucker conditions in nonlinear programming. *European Journal of Operational Research, 180*(1), 479–484.

Blahovec, J. (2008). *Agromaterials*. Prague: Czech University of Life Sciences Prague.

Blahovec, J., & Řezníček, R. (1980). *Fractionation of the forage*. Prague: Czech University of Life Sciences Prague.

Connelly, R. K., & Kokini, J. L. (2003). 2-D numerical simulation of differential viscoelastic fluids in a single-screw continuous mixer: application of viscoelastic FEM methods. *Advances in Polymer Technology, 22*(1), 22–41.

Connelly, R. K., & Kokini, J. L. (2007). Examination of the mixing ability of single and twin screw mixers using 2D FEM simulation with particle tracking. *Journal of Food Engineering, 79*, 956–969.

Dekys, M., & Broncek, O. (2012). Measuring strain of the lattice towers. *Communications: Scientific Letters of the University of Zilina, 14*(3), 39–42.

Dobrzanski, B., & Stepniewski, A. (2013). Physical properties of seeds in technological processes, . In *Advances in agrophysical researchAgricultural and biological sciences*http://dx.doi.org/10.5772/56874 (Chapter 11).

Emin, M. A., & Schuchmann, H. P. (2013). Analysis of the dispersive mixing efficiency in twin-screw extrusion. *Journal of Food Engineering, 115*, 132–143.

Fomin, V. I. (1978). *Vlažnoje frakcionirovanije zeljonych kormov* [*Wet fractionation of green forage*] (160 pp.). Rostov on Don: Izdatelstvo Rostovskovo Universiteta.

Geng, J., Howell, D., Longhi, E., & Behringer, R. P. (2001). Foot prints in sand: the response of a granular material to local perturbations. *Physical Review Letters, 87*(3), 035506-1/4.

Harewood, F. J., & McHugh, P. E. (2007). Comparison of the implicit and explicit finite element methods using crystal plasticity. *Computational Materials Science, 39*, 481–494.

Hedjazia, L., Martin, C. L., Guessasma, S., Della Valle, G., & Dendievel, R. (2012). Application of the discrete element method to crack propagation and crack branching in a vitreous dense biopolymer material. *International Journal of Solids and Structures, 49*(13), 1893–1899.

Herak, D., Gurdil, G., Sedlacek, A., Dajbych, O., & Simanjuntak, S. (2010). Energy demands for pressing *Jatropha curcas* L. seeds. *Biosystems Engineering, 106*(4), 527–534.
Herak, D., Kabutey, A., Divisova, M., & Simanjuntak, S. (2013). Mathematical model of mechanical behaviour of *Jatropha curcas* L. seeds under compression loading. *Biosystems Engineering, 114*(3), 279–288.
Herak, D., Kabutey, A., Divisova, M., & Svatonova, T. (2012). Comparison of the mechanical behaviour of selected oilseeds under compression loading. *Notulae Botanicae Horti Agrobotanici, 40*(2), 227–232.
Herak, D., Kabutey, A., & Hrabe, P. (2013). Oil point determination of *Jatropha curcas* L. bulk seeds under compression loading. *Biosystems Engineering, 116*(4), 470–477.
Herak, D., Kabutey, A., Petru, M., Hrabe, P., Lepsik, P., & Simanjuntak, S. (2014). Relaxation behaviour of *Jatropha curcas* L. bulk seeds under compression loading. *Biosystems Engineering, 125*, 17–23.
Hinton, M. J., Kaddour, A. S., & Soden, P. D. (2004). *Failure criteria in fibre-reinforced-polymer composites. The world-wide failure exercise* (p. 1255). All rights reserved: Elsevier Ltd..
Kabas, O., Celik, H. K., Ozmerzi, A., & ˙Akinci, I. (2008). Drop test simulation of a sample tomato with finite element method. *Journal of the Science of Food and Agriculture, 88*, 1537–1541.
Kabutey, A., Herák, D., Chotěborský, R., Dajbych, O., Divišová, M., & Boatri, W. E. (2013). Linear pressing analysis of *Jatropha curcas* L. seeds using different pressing vessel diameters and seed pressing heights. *Biosystems Engineering, 115*(1), 43–49.
Karaj, S., & Müller, J. (2010). Determination of physical, mechanical and chemical properties of seeds and kernels of *Jatropha curcas* L. *Industrial Crops and Products, 32*, 129–138.
Karaj, S., & Müller, J. (2011). Optimizing mechanical oil extraction of *Jatropha curcas* L. seeds with respect to press capacity, oil recovery and energy efficiency. *Industrial Crops and Products, 34*, 1010–1016.
Khan, L. M., & Hanna, M. A. (1983). Expression of oil from oilseeds – a review. *Journal of Agricultural Engineering Research, 28*, 495–503.
Koegel, R. G., Fomin, V. I., & Bruhn, H. D. (1973). Roller maceration and fractionation of forage. *Transactions of the ASAE, 16*, 236–240.
Krajcinovic, D. (1996). Damage mechanics. In *North-Holland series in applied mathematics and mechanics*. Elsevier Science B.V.
Legras, J. (1956). *Techniques de résolution des équations aux dérivées partielles*. Paris: Dunod.
Lim, S., Hoong, S. S., Teong, L. K., & Bhatia, S. (2010). Supercritical fluid reactive extraction of *Jatropha curcas* L. seeds with methanol: a novel biodiesel production method. *Bioresource Technology, 102*, 7169–7172.
Ma, F., Cholewa, E., Mohamed, T., Peterson, C. A., & Gijzen, M. (2004). Cracks in the palisade cuticle of soybean seed coats correlate with their permeability to water. *Annals of Botany, 94*, 213–228.
Makkar, H. P., Francis, G., & Becker, K. (2008). Protein concentrate from *Jatropha curcas* screw-pressed seed cake and toxic and antinutritional factors in protein concentrate. *Journal of the Science of Food and Agriculture, 88*, 1542–1548.
Metzgera, D., Jarrett, N. K., & Dantziga, J. (2001). A sand surface element for efficient modeling of residual stress in castings. *Applied Mathematical Modelling, 25*(10), 825–842.
Petrakis, E., & Dobry, R. (1989). *Micromechanical behavior and modelling of granular soil*. Report AFOSR 89-1229. New York: Rensselaer Polytechnic Institute.
Petrakis, E., Dobry, R., & Ng, T. (1988). *Small strain response of random arrays of elastic spheres using a non-linear distinct element procedure*. Report AFOSR 89-1229. New York: Rensselaer Polytechnic Institute.
Petrů, M., & Novák, O. (2010). Mechanical properties measurement and comparison of polyurethane foam substitute. *ACC Journal, Issue A, Natural Sciences and Technology, 16*(1), 50–59.
Petrů, M., Novák, O., Herák, D., & Simanjuntak, S. (2012). Finite element method model of the mechanical behaviour of *Jatropha curcas* L. seed under compression loading. *Biosystems Engineering, 111*(4), 412–421.
Petrů, M., Novák, O., & Lepšík, P. (2014). Analysis and measurement of the charge intensity of the selected electrospinning electrodes. *Applied Mechanics and Materials, 486*, 217–222.
Petrů, M., Novák, O., Ševčík, L., & Lepšík, P. (2014). Numerical and experimental research of design optimization of baths for the production of nanofibers by the electrospinning. *Applied Mechanics and Materials, 486*, 157–162.
Petrů, M., Novák, O., Vejrych, D., & Lepšík, P. (2013). FEM study of the strain kinematics in the 3D nanofibrous structure prepared by the electrospinning process. *Applied Mathematics, 4*(5a), 80–90.
Raji, A. O., & Favier, J. F. (2004). Model for the deformation in agricultural and food particulate materials under bulk compressive loading using discrete element method. I: theory, model development and validation. *Journal of Food Engineering, 64*, 359–371.
Rong, G., Negi, S. C., & Jofriet, J. C. (1995). Simulation of the flow behaviour of bulk solids in bins. Part 2: shear bands, flow, corrective inserts and velocity profile. *Journal of Agricultural Engineering Research, 62*, 257–269.
Samonds, M., Morgan, K., & Lewis, R. W. (1985). Finite element modelling of solidification in sand castings employing an implicit–explicit algorithm. *Applied Mathematical Modelling, 9*(3), 170–174.
Sathar, S., Worden, R. H., Faulkner, D. R., & Smalley, P. C. (2012). The effect of oil saturation on the mechanism of compaction in granular materials: higher oil saturation lead to more grain fracturing and less pressure solution. *Journal of Sedimentary Research, 82*(8), 571–584.
Stefan, B. S., Ionescu, M., Voicu, G., Ungureanu, N., & Vladut, V. (2013). Calculus elements for mechanical presses in oil industry. In I. Muzzalupo (Ed.), *Agricultural and biological sciences "food industry", book*http://dx.doi.org/10.5772/53167.
Sukumaran, C. R., & Singh, B. P. N. (1989). Compression of a bed of rapeseeds: the oil-point. *Journal of Agricultural Engineering Research, 42*, 77–84.
Vyakaranam, K. V., & Kokini, J. L. (2011). Advances in 3D numerical simulation of viscous and viscoelastic mixing flows. In J. M. Aguilera, et al. (Eds.), *Food engineering seriesFood engineering interfaces*. Springer Science+Business Media.
Wang, S., Zheng, H., Li, Ch, & Ge, X. (2011). A finite element implementation of strain-softening rock mass. *International Journal of Rock Mechanics and Mining Sciences, 48*(1), 67–76.
Zeng, Z., & Grigg, R. (2006). A criterion for non-Darcy flow in porous media. *Transport in Porous Media, 63*, 57–69.
Zhong, Z. H. (1993). *Finite element procedures for contact – Impact problems*. Oxford: Oxford University Press.